Journal of Magnetism and Magnetic Materials 321 (2009) 3520–3525

Contents lists available at ScienceDirect

Journal of Magnetism and Magnetic Materials

journal homepage: www.elsevier.com/locate/jmmm

Experiments on breakups of a magnetic fluid drop through a micro-orifice

Ching-Yao Chen [a,*], C.-H. Chen [b], W.-F. Lee [c]

[a] Department of Mechanical Engineering, National Chiao Tung University, Taiwan, R.O.C.
[b] Department of Automation Engineering, Nan-Kai University of Technology, Taiwan, R.O.C.
[c] Department of Mechanical Engineering, National Yunlin University of Science and Technology, Taiwan, R.O.C.

ARTICLE INFO

Article history:
Received 29 October 2008
Received in revised form
16 April 2009
Available online 26 June 2009

Keywords:
Ferrofluid
Drop breakup
Surface tension

ABSTRACT

We experimentally study the breakups of a ferrofluid drop passing through a narrow passage under the attraction of an external field. After passing through the orifice, the fluid thread starts to neck down significantly and eventually breaks to form new droplets. The dynamics of the ferrofluid breakup are analyzed parametrically, including the diameter of the orifice and the local field strength. The patterns of fluid breakups can be characterized by two measurements of the breaking droplets, such as their sizes and stretching lengths. These two characteristic measurements mainly depend on the diameter of the orifice. Breaking droplets with less stretching and smaller sizes are resulted from a narrower orifice. On the other hand, the number of total breaking droplets that represents the transport effectiveness of ferrofluids significantly depends on both the diameter of the orifice and the local field strength. While a stronger field generates more breaking droplets, a maximum number of breaking droplets occurs at an intermediate orifice's diameter.

1. Introduction

Ferrofluids are colloidal suspensions of single-domain magnetic nano-particles coated by a layer of surfactants in a carrier liquid, such as water or oil. They were first developed in the 1960s as bearing seals for space applications. Ferrofluids applied in multistage rotary seals, inertial dampers and loudspeakers had been well-established goods in the industry [1–3]. New applications are implemented in the domain of micro-technology developed for biomedical purposes. For the applications of such a problem, magnetically actuated plugs of ferrofluid are used to design microfluidic valves and pumps. Typical examples are referred to Refs. [4,5]. In general, a series of electromagnets are applied to generate a magnetic field gradient that moves the ferrofluid to pump the liquid in a capillary tube or channel. Another possible application is to produce medical solutions in the form of magnetic fluid. With guidance by an external magnetic field, the medication can reach and remain at the target spot, which is hard to achieve for traditional human circulation. Ganguly et al. [6] analyzed the ferrofluid transport for magnetic drug targeting (MDT). They experimentally and numerically investigated the magnetically induced accumulation of ferrofluid at target location and its subsequent dispersion in a steady host fluid flow. For further development of such applications, numerous relevant studies on the transport and fluid dynamics of ferrofluids in a tube under the influence of an applied magnetic field have been presented. Fluid transports and dynamics of ferrofluids under various field and flow conditions in a fully miscible environment are examined to understand the interactions of magnetization and concentration diffusion [7–11]. In addition, the fundamental problem regarding the dynamics of a magnetic drop, such as deformation, pinch-off and breakup, plays an important role in transport of ferrofluids. The phenomena of drop breakup for a non-magnetic bubble or drop have been studied intensively for several decades [12] and are still active ongoing subjects in recent years [13–15]. A detailed review of drop breakup is presented by Eggers [12]. Furthermore, the breakup and coalescence of polymer drops in an immiscible polymeric fluid are also investigated carefully due to potential applications. Recent developments of this complex fluids system are presented by Leal [16]. On the other hand, studies regarding the breakup dynamics of a ferrofluid drop under the influences by an external field are less comprehensive. Several researchers [17–22] calculated the static shape of a magnetic fluid drop in a homogeneous magnetic field by different theoretical approaches. They studied the stretched shape [17–20] or the breakup [21,22] of a magnetic fluid drop under the influence of an applied magnetic field as well as the interactions and deflections of two magnetic functional fluid drops in a magnetic field. A more relevant experiment regarding the breakup of a ferrofluid bridge under an external field has also been performed [23]. Detail temporal evolutions of breakups are recorded and analyzed to make a comparison with a universal theorem. In this experimental study, the interesting dynamics and morphologies of a ferrofluid drop through a narrow

* Corresponding author.
E-mail address: chingyao@mail.nctu.edu.tw (C.-Y. Chen).

0304-8853/$ - see front matter © 2009 Elsevier B.V. All rights reserved.
doi:10.1016/j.jmmm.2009.06.066

passage under the effects of an applied magnetic field are presented. In addition, quantitative measurements of interests will also be obtained and analyzed.

2. Experimental apparatuses

A schematic of the experimental apparatus is shown in Fig. 1. A ferrofluid drop is first placed in a quartz tube. The quartz tube of 6.0 mm inner diameter and 8.0 mm outer diameter is horizontally supported by a coil of electromagnet. Each end of the quartz tube was connected to a flexible tube with an open end to keep the same level of the free surface. The electromagnetic coil, consisting of 1500 turns of 0.6-mm-diameter wire, is 41.0 mm in width with an 8.1-mm-diameter central hole. A 3.0 mm short tube type acrylic orifice of an inner diameter d is fixed firmly inside the quartz tube. The ferrofluid used is a commercial light mineral oil-based ferrofluid (EMG905) produced by Ferrotec Corporation, with a saturation magnetization $Ms = 400$ G, a viscosity $\eta = 9$ cp, a surface tension $\sigma = 25.6$ dyn/cm and a density $\rho = 1.24$ gm/ml, respectively. The tube is filled with distilled water–glycerol mixture (viscosity $\eta \approx 48.5$ cp) to closely match the density of ferrofluid. To avoid the adhesion of ferrofluid drop to the solid, Tween-80 is used to lubricate the surface of the quartz tube and the acrylic orifice. A positive-displacement microliter system is used to inject ferrofluids with a constant volume of 17 μl into the tube to form a drop. The ferrofluid drop is drawn by a permanent magnet to 15 mm upstream of the orifice's entrance before the experiment starts.

The coil of electromagnet is fixed at a distance l downstream of the exit of the orifice. The distributions of magnetic field strengths H in the axial-direction for different current strengths applied in the experiments are measured with a transversal gauss probe (SYPRIS-6010). They appear to have a similar profile to the experimental measurements in Ref. [24] for $z \leq 30$ mm, where z stands for the distance away from the center of the coil. However, at $z > 30$ mm the fields decay more slowly. The distributions of the fields can be represented by the appropriate curves expressed as $H = H_0 \exp(-0.0018z^2)$ at $z \leq 30$ and $H = H_0 \exp(-0.054z)$ at $z > 30$, where H_0 is the maximum magnetic field strength at the center of the coil ($z = 0$). By the present notation, location of the coil's edge is at $z = 20.5$ mm (half width of the coil) with its corresponding local field strength denoted as H_c. We would like to point out that the above expressions do not satisfy the Maxwell equation, and are merely numerical estimations for better understanding the distribution profiles. Nevertheless, the field strengths of actual measurements are used in later sections. As for the magnitude of radial component, it is found to be significantly smaller than its axial counterpart and neglected in the following discussion.

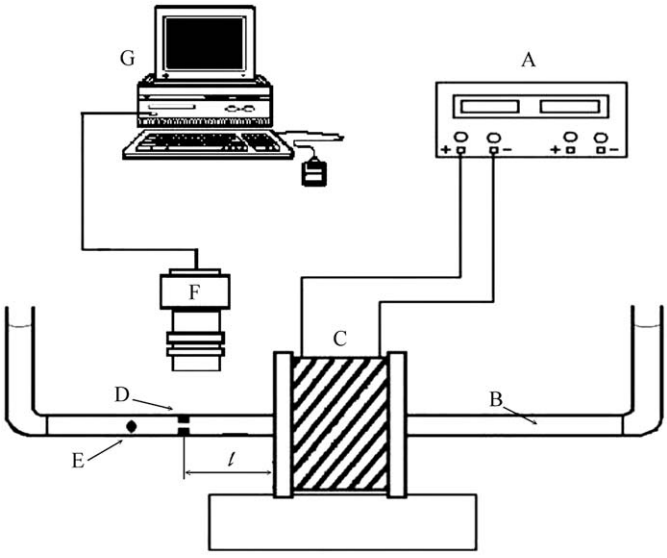

Fig. 1. Schematic presentation of the experimental apparatus: (A) power source; (B) glycerol–water mixture; (C) coil; (D) acrylic orifice; (E) ferrofluid drop; (F) CCD-camera and (G) personal computer.

When the magnetic field is triggered, the ferrofluid drop is attracted and moves through the orifice. The motion and deformation of ferrofluid drop is observed and recorded by a high-speed video camera system (PULNiX TM-6740GE). The system is capable to record 200 frames per second. The images are subsequently analyzed on a personal computer. In this study, the influences of the orifice's diameter (d), coil distance to the orifice's exit (l) and the strength of the local magnetic field (H_c) to the motion and deformation of the drop are investigated.

3. Results and discussion

3.1. Description of droplet breakup

A representative case of $d = 0.5$ mm, $H_c = 510$ Oe and $l = 10$ mm is first described as the sequential snapshots shown in Fig. 2. At $t = 0$ s, the magnetic drop is drawn to 15 mm upstream of the orifice's entrance and stays at the bottom of the quartz tube. Because of gravitational force induced by the slight density difference and a relatively weaker surface tension between the ferrofluids and water–glycerol mixture, the drop appears distorted initially. When the magnetic field is triggered, a magnetic force immediately acts on the magnetized drop. The drop deforms slightly and moves ahead ($t = 1.96$ s) until it runs into the entrance of the orifice in a fraction of a second at $t = 2.27$ s. Even the resistance caused by viscous drag and surface tension increases significantly inside the orifice, the magnetic attraction is still strong enough to move the ferrofluids forward. The drop is

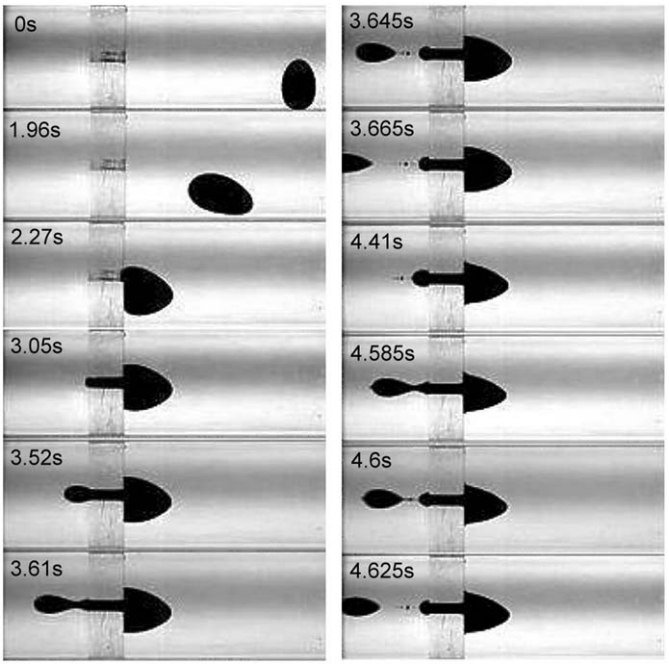

Fig. 2. Sequential images of the drop motion for the representative case of $d = 0.5$ mm, $H_c = 510$ Oe and $l = 10$ mm at different times.

jammed into the orifice at $t = 3.05$ s. While the drop keeps stretching forward to form a fluid thread, part of the thread extends through the orifice with a rounded leading edge. Consequently, the drop begins to neck during $t = 3.52$ to 3.61 s, and the fluid eventually breaks into a new droplet at $t = 3.645$ s and keeps being attracted forward ($t = 3.665$ s). The remaining part of the fluid thread appears a conical end and springs back due to a significant constraint of surface tension. A more detailed morphologies of the necking and breakup process can be referred to Ref. [23]. After the first breakup, similar process occurs in which the remaining part of the fluid thread is prolonged to pass through the orifice ($t = 4.41$ s) and neck again ($t = 4.585$ s). This leads to the formation of another breaking droplet to travel toward the coil at $t = 4.6$ s. The breakups occur continually until a few residual fluids are jammed inside the orifice. Nine fully breaking droplets, denoted as $N = 9$, are identified for this representative case.

These interesting fluid breakups are mainly due to interaction among the attracting magnetic force and resistant viscous cohesion and surface tension. While the magnetic force tends to pull the ferrofluid thread through the orifice, the viscous cohesion and surface tension act oppositely. In addition, the fluid thread subjects a stronger magnetic attraction as its front moves closer to the coil under the present field distribution. As a result, the breakup would eventually occur at a location where the resistant viscous cohesion and surface tension are no longer able to sustain an equilibrium. Another interesting feature is the formation of satellite droplets. When the fluid thread breaks up, the front part of the thread moves forward slowly and the rear part bounces back rapidly until the two ends join and form satellite droplets at $t = 3.645$ and 3.665 s. This phenomenon was also commonly observed in the breakup of jets [25] and the pinch-off of a pendant drop [26] as well as the similar breakup of a ferrofluid bridge [23]. In order to quantitatively describe the fluid breakup, we denote the distances of the ferrofluid thread's front away from the orifice's exit as the front positions (L_d). The front positions immediately before ($t = 3.61$ s) and after ($t = 3.645$ s) the occurrence of breakup are referred to as L_{db} and L_{dp}, respectively. They are measured as $L_{db} = 5.4$ mm and $L_{dp} = 0.7$ mm in the present representative case. These measurements will be applied for the quantitative analysis presented in the next paragraph.

It is noteworthy to compare the present device with the similar experiments mounted vertically so that the fluids are subjected to a gravitational attraction. Even the somehow similar fluid breakups might be produced under a sufficient gravitational force, the current device is much more effective in the manipulation of fluids. Apparently, the first advantage would be a controllable magnitude of the external field strength, so that one can obtain desired fluid behavior, such as the number of breaking droplet. Another main difference is a more efficient breakup process due to the spatial variation of local magnetic attraction. In a gravitational driving case, the gravity acting to the fluids remains constant for the whole process. On the other hand, because of the field distribution, the magnetic attraction is greater as the fluids getting closer to the coil. This spatial variation would provide additional stretching effects and result in more effective breakups.

Next, we examine the role played by the diameter of the orifice. As shown in Fig. 3, the strength of the magnetic field is kept at $H_c = 510$ Oe, but the inner diameter of orifice is varied to $d = 0.3$ mm (left column) and $d = 0.8$ mm (right column), respectively. It is understandable that a larger viscous drag is generated in a smaller passage. In addition, a smaller orifice leads to a larger curvature of the fluid thread and results in a stronger resistance of surface tension as well. Consequently, the ferrofluid would be more difficult to travel through the orifice. Shown in the left column of Fig. 3, the ferrofluid drop is observed to pass through a small orifice of $d = 0.3$ mm slowly as one would expect.

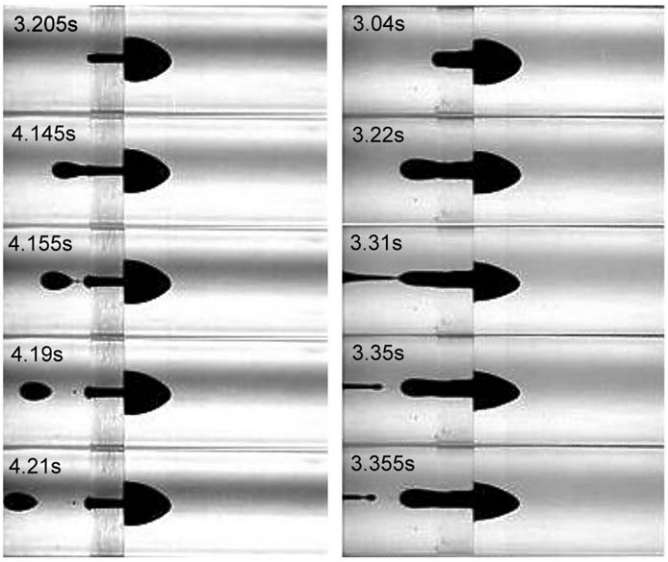

Fig. 3. Sequential images of drop motion for different diameters of $H_c = 510$ Oe and $l = 10$ mm; left column: $d = 0.3$ mm; right column: $d = 0.8$ mm.

The ferrofluid initially reaches the exit of the orifice at a later time $t = 3.205$ s. By the same token, processes of necking and pinch-off breakup of the fluid thread occur at later times of $t = 4.145$ and 4.155 s, respectively. The breakup occurs at a position closer to the exit of the orifice (a lower value of $L_{db} = 3.6$ mm). As a result, the breaking droplet appears smaller in size. Besides, a smaller number of fully evolved breaking drops ($N = 5$) point out a less prominent thread breakup. On the other hand, the whole process takes place faster for a larger diameter of $d = 0.8$ mm, as shown in the right column of Fig. 3. The arrival to the exit, necking and pinch-off of the drop occur at earlier times of $t = 3.04$, 3.31 and 3.35 s, respectively. The location where fluid thread breakup occurs is further away from the exit (a higher value of L_{db}), in which is beyond the maximum observing range. Meanwhile, the significant fluid stretch is observed. It is noteworthy for an even larger diameter of $d = 1.0$ mm, the drop deforms into two blobs connected by a thread and quickly passes the narrow orifice without any breakups.

Effects of the strength of the magnetic field are also experimented. The local field strengths can be varied either by a different characteristic field strength H_c or a different coil distance l. The cases of a weaker local field strength, compared to the representative case shown in Fig. 2, are shown in Fig. 4, such as the cases of $H_c = 464$ Oe with $l = 10$ mm and $H_c = 557$ Oe with $l = 15$ mm in the left and right column, respectively. Compared to the representative cases in a stronger magnetic field shown in Fig. 2, the drop moves significantly more slowly. Nevertheless, it is interesting to notice that the patterns of initial thread breakup shown in Fig. 4 remain quite similar regardless of the magnitudes of the local field. This suggests the patterns of the fluid breakup are hardly affected by the variation of local field strength based on qualitatively visual inspection.

3.2. Parametric investigation

As the qualitative observations presented in the previous section, a few preliminary arguments can be made as: (i) the patterns of breakups, which can be characterized by the sizes of breaking droplets and locations of breakups (L_{db} and L_{dp}), depend strongly on the orifice's diameters but insignificantly on the local field strengths; (ii) the traveling speeds as well as the breaking process of the ferrofluid drop and numbers of fully evolved

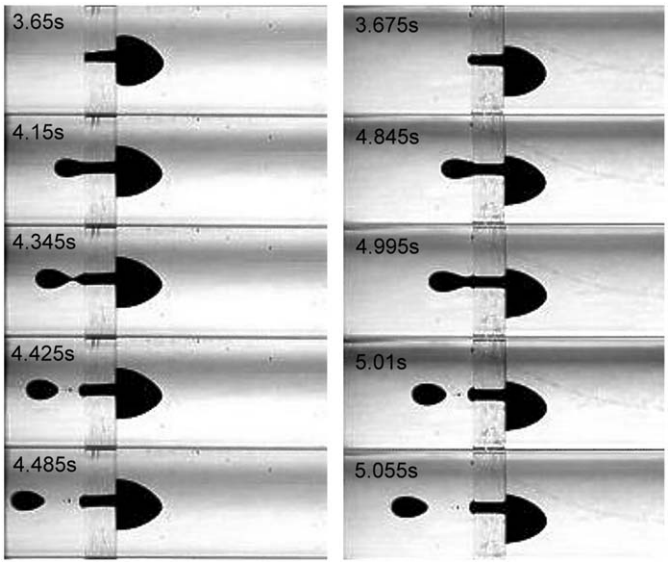

Fig. 4. Sequential images of drop motion for different field strength of $d = 0.5$ mm; left column: $H_c = 464$ Oe and $l = 10$ mm; right column: $H_c = 557$ Oe and $l = 15$ mm.

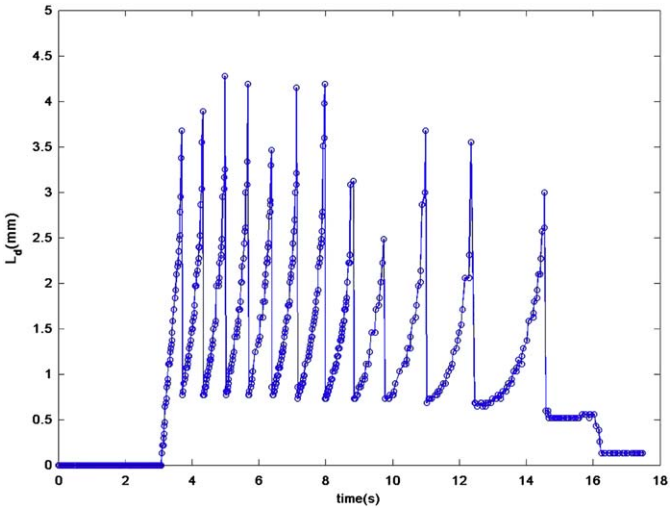

Fig. 5. Time evolution of the droplet's front position L_d (distance of ferrodrop's front away from the exit of the orifice) for $H_c = 557$ Oe, $l = 10$ mm and $d = 0.3$ mm.

breaking droplets are affected significantly by both the local field strengths and the diameters of orifices. To better understand these measurements and the mechanisms at work, a more quantitative discussion is presented in this section.

Fig. 5 shows the detailed evolution of the distance of fluid thread's front position L_d for a typical case of $H_c = 557$ Oe, $l = 10$ mm and $d = 0.3$ mm. Some important numbers and locations can be easily identified by this figure. The ferrofluid thread attracted by the magnetic field first reaches the orifice's exit at $t = 3.03$ s, and start to be stretched away ($L_d > 0$). The fluid thread reaches a local maximum stretching distance of $L_{db} = 3.68$ mm at $t = 3.585$ s before thread breakup, followed by a sudden withdrawal to a local minimum distance of $L_{dp} = 0.77$ mm at $t = 3.6$ s after the breakup. Similar processes of stretches and breakups occur repeatedly until $t = 14.58$ s. Because of extreme sensitivity to the recoding timings, significant fluctuations of the front positions before breakup, ranging from $L_{db} = 4.28$–2.48 mm, are measured within the entire observation. By contrast, the front positions post-breakup are located more closely around $L_{dp} = 0.78$ mm. We use the front difference before and post the drop breakups, $\Delta L_d = L_{db} - L_{dp}$, to represent the stretching length of the breaking droplet. The mean stretching length for this particular experiment is obtained as $\Delta L_d = 3.34$ mm. As to the number of breaking droplets (N), which is relevant to the effectiveness of fluid transport, it can be easily obtained as $N = 12$ by counting the number of peaks. We perform the similar analysis to all the experiments, and the corresponding measurements are then obtained accordingly.

Fig. 6 displays the front positions for various values of the control parameters, including d, H_c and l. Two apparent distributions, distinguished by the values of d, are observed. For the same value of d regardless their correspondent values of H_c and l, the variations of all the lengths, for example, L_{db}, L_{dp} and ΔL_d, among different rounds of experiments are quite insignificant. On the other hand, higher values of these interested lengths are observed for a bigger orifice's size. Another quantity regarding the patterns of breakup is the volume of the individual breaking droplet. Again, the sizes of breaking drops are strongly affected by the diameter of the orifice. The volume (V) is represented by the first breaking droplet and plotted in Fig. 7 vs. d. It is expected that a bigger breaking droplet would result from a larger orifice's diameter. The above results indicate the features of breaking patterns are more dominated by the size of orifice at the present situations, rather than the external magnetic field. This fact is consistent with the qualitative observations stated in the previous section. Other measurement of interests relevant to the effectiveness of transporting the ferrofluids through the orifice is the total number of breaking droplets (N). The total number of breaking droplets (N) at various experimental conditions is shown in Fig. 8. It is apparent that N depends strongly on both the local magnetic field strength and the orifice's size. For a fixed orifice's diameter, more breaking droplets result from a stronger local field strength. As shown in Fig. 8 for $d = 0.5$ mm, only a single breakup ($N = 1$) occurs at $H_c = 557$ Oe and $l = 15$ mm. With the increase in the local magnetic field strength by shortening the coil distance to $l = 10$ mm, the mean numbers of breaking droplets increase to nearly $N = 12$. A similar trend is found for a smaller diameter of $d = 0.3$ mm. Nevertheless, the highest number of breaking droplets are formed in an intermediate diameter of $d = 0.5$ mm if the field condition remained the same.

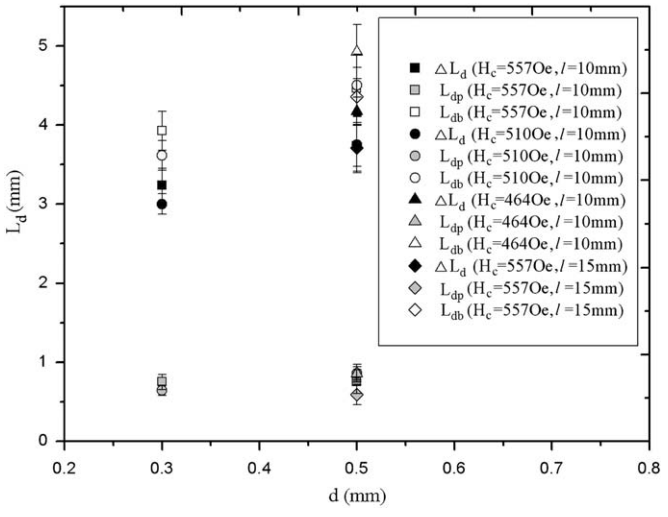

Fig. 6. Front positions before (L_{db}) and post (L_{dp}) the drop breakup and stretching lengths (ΔL_d) for various values of the orifice's diameter d, the field strength H_c and the coil distance l. For the same value of d regardless of their correspondent values of H_c and l, the variations of all the front positions among different rounds of experiments are quite insignificant.

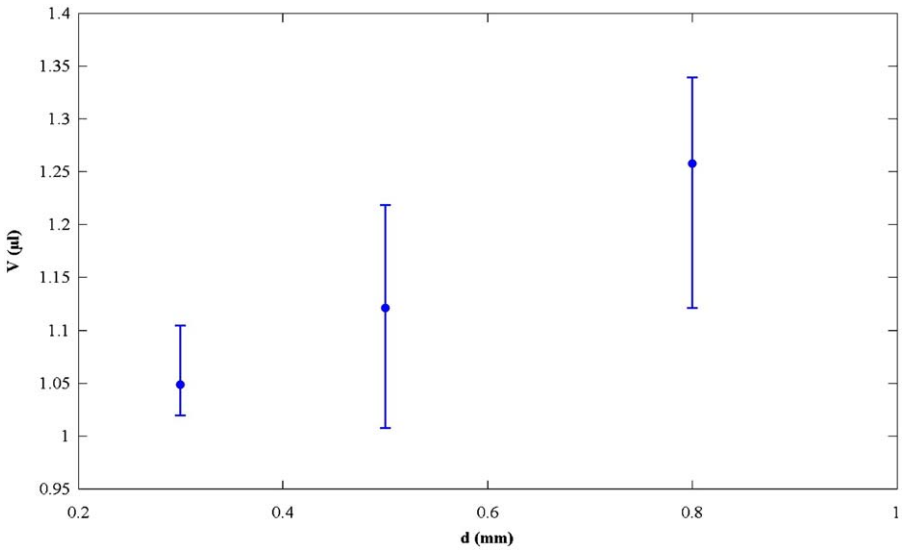

Fig. 7. Volume of breaking droplets V for various sizes of the orifice's diameter d at $H_c = 557$ Oe and $l = 10$ mm. A bigger breaking droplet results from a larger orifice.

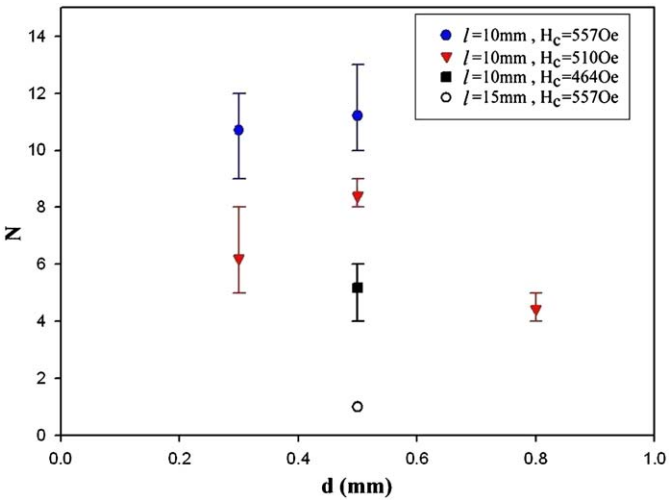

Fig. 8. Number of breaking droplets N for various conditions of the orifice's diameters d, the field strengths H_c and the coil distance l. Number of breaking droplets significantly depends on all the parameters. More breaking droplets result from a larger local field strength and an intermediate orifice size.

Dominance of the orifice's size to the breaking patterns as stated in the previous paragraph, determined by the stretching length (ΔL_d) and the volume of the first breaking droplet (V), can be understood by the viscous breakups of thread. Since the dominant breaking mechanism is mainly determined by the surface tension and viscous cohesion at the present situation [27–29], so that a strong dependence on the diameter of the orifice is expected. On the other hand, major effects of local field strengths are to drive the fluid motion. As a result, the correlation between the breaking patterns and the field strength is insignificant. In addition, a smaller size of the orifice implies both stronger viscous cohesions and surface tension constraints, so that thread advancing velocity is slower. In addition, a smaller diameter forms a thinner fluid thread whose breakup is more easily to occur. The slower advancing velocity associated with a thinner body of the fluid thread explain that a less stretching (a shorter ΔL_d) is resulted from a smaller diameter. On the other hand, a stronger local field strength naturally provides a larger net attracting force if the size of the orifice is fixed, so that more ferrofluids can be attracted toward the coil. Meanwhile, the volume of an individual breaking droplet is smaller for a smaller orifice's diameter regardless the field strength as discussed above. Consequently, a higher number of breaking droplets are formed for a stronger field under the same size of orifice. As to the correlation between the number of breaking droplet and the diameter of the orifice in the same field condition is a bit more complex. For a fixed value of the magnetic field strength, a larger amount of ferrofluids can effectively pass through the bigger orifice because of less induced viscous drag and surface tension constraint. Nevertheless, a bigger orifice's diameter would lead to the formation of bigger breaking droplets. These two opposite behaviors result in a maximum number of breaking droplets at an intermediate diameter of $d = 0.5$ mm. These results explain both the field strengths and the diameters of the orifice are important in considering the number of breaking droplets.

4. Concluding remarks

We present an experimental study on the breakup instability of a ferrofluid drop. The experiments have shown the process of a ferrofluid drop passing through a narrow passage under an applied magnetic field. Interesting fluids breakups are observed. To quantitatively describe the patterns of breakups and the effectiveness of ferrofluid transport through the orifice, characteristic measurements of the breaking droplets, such as their stretching lengths, sizes and numbers, are documented systematically and analyzed against three important control parameters, e.g. the magnetic field strength H_c, the diameter of the orifice d and the coil distance to the orifice l. The patterns of drop breakups can be characterized by volumes and stretching lengths of breaking droplets. It is found that both the volume V and stretching lengths ΔL_d of breaking droplets are mainly determined by the diameter of the orifice, regardless of magnitudes of the local magnetic field strength. Smaller breaking droplets with less stretching are resulted from a smaller diameter of the orifice because of the stronger viscous resistance and surface tension constraint. However, the transport effectiveness of ferrofluids through the orifice, which can be represented by the number of total breaking droplets N, significantly depends on both the

orifice's diameter and the field strength. While a stronger field generates more breaking droplets, a maximum number of breaking droplets occurs at an intermediate orifice's diameter ($d = 0.5$ mm at the present experimental condition) due to its favorable intermediate behaviors of orifice's resistances and volume of breaking droplet as well.

Acknowledgement

C.-Y. Chen thanks the National Science Council of the Republic of China for financial support of this research through grant NSC 94-2212-E-224-011. C.-H. Chen is supported by NSC 97-2221-E-252-017.

References

[1] R.E. Rosensweig, Ferrohydrodynamics, Cambridge University Press, New York, 1985.
[2] K. Raj, B. Moskowitz, R. Casciari, J. Magn. Magn. Mater. 149 (1985) 174–180.
[3] B. Berkovsky, V. Medvedev, M. Krakov, Magnetic Fluids Engineering Applications, Oxford University Press, New York, 1993.
[4] H. Hartshorne, C.J. Backhouse, W.E. Lee, Sensors Actuators B 99 (2004) 592–600.
[5] L. Love, J. Jansen, T. McKnight, Y. Roh, T. Phelps, IEEE Trans. Nanobioscience 3 (2) (2004) 101–110.
[6] R. Ganguly, A.P. Gaind, S. Sen, I.K. Puri, J. Magn. Magn. Mater. 289 (2005) 331–334.
[7] R. Ganguly, A.P. Gaind, Phys. Fluids 17 (2005) 057103.
[8] R. Ganguly, B. Zellmer, I.K. Puri, Phys. Fluids. 17 (2005) 097104.
[9] C.-Y. Chen, C.-Y. Liao, Int. J. Numer. Methods Heat Fluid Flow 13 (2) (2003) 244–261.
[10] C.-Y. Chen, C.-Y. Hong, L.-M. Chang, Fluid Dyn. Res. 32 (2003) 85–98.
[11] C.-Y. Chen, H.-C. Lin, W.-K. Tsai, C.-H. Lin, J. Mech. 24 (2008) 311–317.
[12] J. Eggers, Rev. Mod. Phys. 69 (865) (1997) 066303.
[13] P. Doshi, I. Cohen, W. Zhang, M. Siegel, P. Howell, O. Basaran, S. Nagel, Science 302 (14) (2003) 1185–1188.
[14] P. Garstecki, H.A. Stone, G.M. Whitesides, Phys. Rev. Lett. 94 (2005) 164501.
[15] S. Quan, J. Hua, Phys. Rev. E 77 (2008) 066303.
[16] L.G. Leal, Studies of Droplet Coalescence and Breakup with Application to Polymer Blending, In: Y. Luo, Q. Rao, Y. Xu (Eds.), Advances In Rheology and Its Applications, 2005, pp. 1–4.
[17] V.I. Arkhipenko, Yu.D. Barkov, V.G. Bashtovoi, Magnetohydrodynamics 14 (3) (1978) 131–134.
[18] J.D. Sherwood, J. Fluid Mech. 188 (1988) 133–146.
[19] O.E. Sero-Guillaume, D. Zouaoui, D. Bernardin, J.P. Brancher, J. Fluid Mech. 241 (1992) 215–232.
[20] H.A. Stone, J.R. Lister, M.P. Brenner, Proc. R. Soc. London A 455 (1999) 329–347.
[21] S. Sudo, A. Nakagawa, K. Shimada, H. Nishiyama, Magnetohydrodynamics 39 (3) (2003) 361–368.
[22] V. Kazhan, V. Korovin, J. Magn. Magn. Mater. 260 (2003) 222–230.
[23] A. Rothert, R. Richter, J. Magn. Magn. Mater. 201 (1999) 324–327.
[24] H. Yamaguchi, I. Kobori, N. Kobayashi, J. Magn. Magn. Mater. 201 (1999) 260–263.
[25] T.A. Kowalewski, Fluid Dyn. Res. 17 (1996) 121–145.
[26] D.M. Henderson, W.G. Pritchard, L.B. Smolka, Phys. Fluids 9 (11) (1997) 3188–3200.
[27] J.R. Lister, H.A. Stone, Phys. Fluids 10 (11) (1998) 2758–2764.
[28] G.H. McKinley, Soc. Rheol. Bull. 74 (2) (2005) 6–9.
[29] C.-Y. Chen, Z.-Y. Cheng, Phys. Fluids 20 (2008) 054105.